

PACS number: 73.63.Bd

**EFFECT OF ANNEALING ON STRUCTURE, MORPHOLOGY,
ELECTRICAL AND OPTICAL PROPERTIES OF NANOCRYSTALLINE
TiO₂ THIN FILMS**

**S.G. Pawar, M.A. Chougule, P.R. Godse, D.M. Jundale, S.A. Pawar,
B.T. Raut, V.B. Patil**

Materials Research Laboratory, School of Physical Sciences,
Solapur University, Solapur-413255, M.S., India
E-mail: drvbpatil@gmail.com

Semi-transparent and highly conducting nanostructured titanium oxide thin films have been prepared by sol-gel method. Thin films of TiO₂ deposited on glass substrates using spin coating technique and the effect of annealing temperature (400 - 700 °C) on structural, microstructural, electrical and optical properties were studied. The X-ray diffraction and Atomic force microscopy measurements confirmed that the films grown by this technique have good crystalline tetragonal mixed anatase and rutile phase structure and homogeneous surface. The study also reveals that the rms value of thin film roughness increases from 7 to 19 nm. HRTEM image of TiO₂ thin film (annealed at 700 °C) shows that a grain of about 50 - 60 nm in size is really aggregate of many small crystallites of around 10 - 15 nm. Electron diffraction pattern shows that the TiO₂ films exhibited tetragonal structure. The surface morphology (SEM) of the TiO₂ film showed that the nanoparticles are fine with an average grain size of about 50 - 60 nm. The optical band gap slightly decreases from 3.26 - 3.24 eV and the dc electrical conductivity was found in the range of 10⁻⁶ to 10⁻⁵ (Ω cm)⁻¹ when the annealing temperature is changed from 400 to 700 °C. It is observed that TiO₂ thin film annealed at 700 °C after deposition provide a smooth and flat texture suited for optoelectronic applications.

Keywords: SOL-GEL METHOD, STRUCTURAL PROPERTIES, OPTICAL PROPERTIES, ELECTRICAL CONDUCTIVITY.

(Received 04 February 2011, in final form 16 March 2011)

1. INTRODUCTION

Many nanostructural materials are now investigated for their potential applications in photovoltaic, electro-optical, micromechanical and sensor devices [1]. Nanoporous TiO₂ thin films for dye-sensitized and ETA (extremely thin absorber) solar cells have been under intense study for many years [2]. The TiO₂ occurs naturally as minerals rutile, anatase and brookite phases. The rutile and anatase phases have been intensively studied and have significant technological uses related in large measure to their optical properties: both are transparent in the visible range and absorb in the near ultraviolet. For the TiO₂ brookite, the width of these domains are depends on the TiO₂ thickness values [3]. The rutile (110) surface is used as a prototypical model for basic studies of oxide surfaces, and is the active component in self-cleaning cement [3]. There is a recent development of interest on transparent rutile n-doped films [4]. At room temperature, the

direct gap energy E_g is 3.06 eV for rutile and is about 3.3 eV for anatase. Mixed-phase TiO_2 material has recently been fabricated by chemical and physical methods, including a sol-gel, hydrothermal, solvothermal, and reactive DC magnetron sputtering method, and has demonstrated excellent photocatalytic activities [5-8]. As usual, the preparation of titanium nanomaterial with two different polymorphs by sol-gel method needs to crystallize the as-prepared titanium hydroxide at high temperature ($\geq 700^\circ\text{C}$). This heat treatment leads to change in the crystallite size as well as morphology of the sol-gel derived titanium oxide [9, 10]. Therefore; the preparation of mixed phase titanium oxide at lower temperature can be useful both in saving energy and getting better properties [11-15]. According to the literature survey, there isn't any study which attempted to systematic investigations viz effect of annealing on structure, morphology, electrical conductivity and band gap of multiphase TiO_2 by sol-gel method.

In the present paper, we report preparation and deposition of nanocrystalline TiO_2 mixed phase (anatase and rutile) thin films by sol-gel spin coating technique. The nanopowders are subsequently sintered at 400 - 700 $^\circ\text{C}$. The nanopowder and films were further investigated for their structural, microstructural and optoelectronic properties.

2. EXPERIMENTAL DETAILS

Nanocrystalline TiO_2 is synthesized by sol-gel method using titanium isopropoxide as a source of Ti. 3.7 ml of titanium isopropoxide was added to 40 ml of methanol and stirred vigorously at temperature 60 $^\circ\text{C}$ for 1 h, this leads to formation of white powder which was sintered at 400 - 700 $^\circ\text{C}$ for 1 h in air to achieve formation of nanocrystalline TiO_2 of 50 - 60 nm size. The nanocrystalline TiO_2 powder was dissolved in *m*-cresol. The solution was stirred for 1 h at room temperature and filtered. A thin film of this filtered nanocrystalline TiO_2 was deposited on a glass substrate by a single wafer spin processor (APEX Instruments, Kolkata, Model SCU 2007). After setting the substrate on the disk of the spin coater, the coating solution approximately 0.2 ml was dropped and spin-coated with 3000 rev. min^{-1} for 40 s in air and dried on a hot plate at 100 $^\circ\text{C}$ for 10 min.

The structural properties of the films were investigated by X-ray diffraction (XRD) (Philips PW - 3710, Holland) using filtered Cu K_α radiation ($\lambda = 1.5406 \text{ \AA}$). High resolution Transmission electron microscopy (HRTEM) and small area electron diffraction (SAED) were obtained in order to investigate the morphology and structure of titanium oxide thin films. The TEM images were taken with a Hitachi Model H-800 transmission electron microscope. In order to determine the particle size and morphology of nanopowder, the annealed powders were dispersed in *m*-cresol and sonicated ultrasonically by using Microclean-103 (OSCAR ultrasonic bath apparatus) to separate out individual particles. The size and morphology of the thin films were then observed on SEM Model: JEOL JSM 6360 operating at 20 kV. Roughness of the film was determined from the Atomic force microscopy (AFM) using (Digital Instruments) Nanoscope III a.

The room temperature dc conductivity measurements were made on thin films using four probe techniques. The optical absorption spectra of TiO_2 thin films were measured using a double-beam spectrophotometer Shimadzu

UV-140 in the 200 - 1000 nm-wavelength range. The thickness of the film was measured by using profilometry using a Dektak profilometer. The values obtained ranged between 100 and 200 nm.

3. RESULTS AND DISCUSSION

3.1 Structural Properties

Fig. 1 shows the X-ray diffraction patterns of nanocrystalline TiO₂ powder annealed at 400 - 700 °C temperatures with a fixed annealing time of 1 h in air. The effect of annealing temperature on the crystallinity of TiO₂ can be understood from the figure.

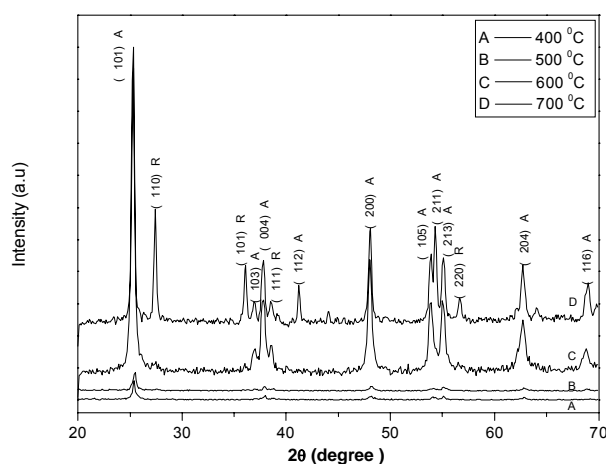


Fig. 1 – X-ray diffraction patterns of TiO₂ nanopowder at different annealing temperatures: (a) 400 °C (b) 500 °C, (c) 600 °C and (d) 700 °C

The X-ray spectra show well-defined diffraction peaks showing good crystallinity. The crystallites are randomly oriented and the d-values calculated for the diffraction peaks are in good agreement with those given in JCPD data card (JCPDS No. 78 – 2485 & 78 – 2486) for TiO₂ anatase and rutile. This means that TiO₂ has been crystallized in a tetragonal mixed anatase and rutile form. These results are in good agreement with other reports on the mixed phase TiO₂ by sol gel method [5-8]. The lattice constants calculated from the present data are $a = 3.7837 \text{ \AA}$ and $c = 9.5087 \text{ \AA}$ respectively. From Fig. 1 it is seen that the (101) peak (anatase phase) of intensity increased with an increase in the annealing temperature. However, the full width at half-maxima FWHM of the (101) peaks was hardly changed with increasing film annealing temperature [9, 10]. The grain size of all TiO₂ samples sintered at 400 °C to 700 °C was calculated using Scherer's equation and it is in the range of 50 - 60 nm, revealing a fine nanocrystalline grain structure.

3.2 Microstructural and morphological properties

AFM (non contact mode) was used to record the topography of the nanocrystalline TiO₂. In this mode, the tip of the cantilever does not contact

the sample surface. The cantilever is instead oscillated at a frequency slightly above its resonance frequency where the amplitude of oscillation is typically a few nanometers (< 10 nm). The surface morphologies of the TiO_2 nanoparticles exhibit notable features. Figures 2 show 2D and 3D AFM images ($3 \mu\text{m} \times 3 \mu\text{m}$) of the TiO_2 nanoparticle films. The average surface roughnesses are in 7 - 19 nm for TiO_2 nanoparticles. The average particle sizes of TiO_2 are found to be in the range of 50 - 60 nm.

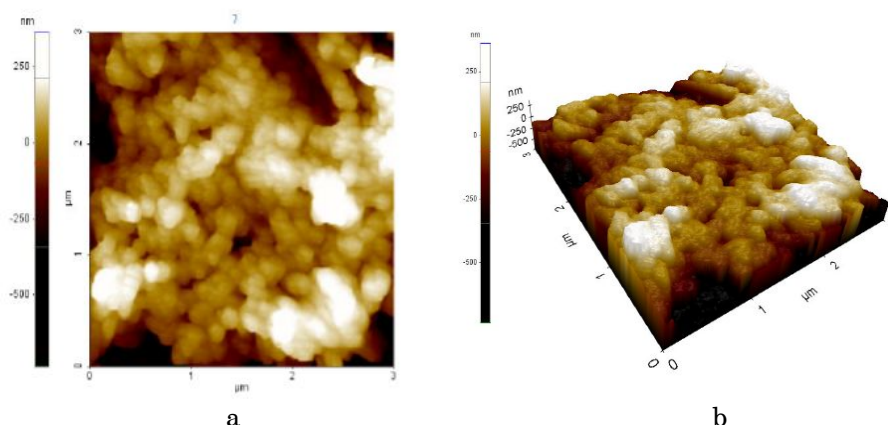


Fig. 2 – AFM images of TiO_2 thin films annealed at 700°C for 1 h in air (a) planer view (b) 3D view

Figure 3 a show high resolution image of titanium oxide thin film annealed at 700°C , recorded from typical regions of films. HRTEM shows a large number of crystalline grains appear in a structured matrix and the grains have a diameter in the range 2 - 3 nm and show lattice spacings of about 0.35 nm. Figure 3 b shows the diffraction patterns obtained from the titanium oxide film annealed at 700°C . The different arrangement of dominant diffracted rings indicates a phase evolution of crystalline grains because of thermal annealing.

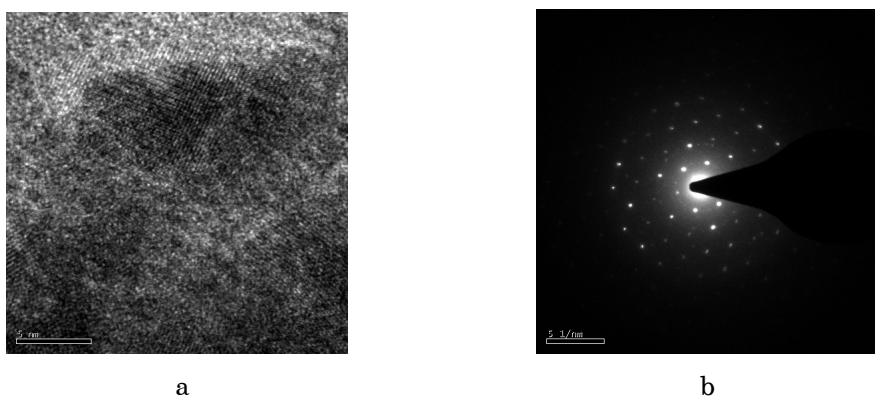


Fig. 3 – TEM of TiO_2 thin film annealed at 700°C for 1 h in air (a) Microstructure (b) Selected Area Electron Diffraction pattern

Table 1 shows the interplanar spacings determined from diffraction pattern together with the corresponding ones of TiO₂ rutile and anatase phases reported in the literature for comparison [9, 10]. It is evident that the film consists of grains having both the interplanar spacings of TiO₂ in the anatase and rutile structural modifications [5-8].

Table 1 – Interplanar spacings deduced from electron diffraction patterns reported in Fig. 3 b together with the corresponding ones obtained from literature data. Numbers in brackets (n) represent the labels of reflections in diffraction patterns.

Interplanar spacings determined titanium oxide films		Interplanar spacings in this work on reported in literature	
(n)	d (nm)	Rutile d (nm) – hkl	Anatase d (nm) – hkl
(1)	0.3551		0.35126 - 101
	0.3242	0.3246 - 110	
		0.25130 - 101	
(2)	0.2371		0.23775 - 004
		0.2187 - 111	
(3)	0.1894		0.18900 - 200
(4)	0.1665		0.16690 - 105
(5)	0.1661		0.16643 - 211
			0.14754 - 204

^aJoint commission Powder Diffraction File No. (78) – 2485 & (78) – 2486)

The film microstructure was studied using Scanning Electron Microscopy. Fig. 4 show the SEM morphology of TiO₂ thin film annealed at different temperatures 400 - 700 °C.

In general, films are homogeneous and continuous separate coating layers are not visible in annealed films. There seems to be mismatch in average size of grains / particles determined through Scherer's calculation utilizing XRD data and SEM analysis .SEM image suggest size of grains to be much larger. Further, while Scherer's calculation suggests an increase in particle size with rise in annealing temperature, SEM images indicate almost a reverse trend. Taking into account the above discrepancy and the fact that SEM analysis reveals formation of particles with different shapes and size, it seems appropriate to consider that the particles which appears in SEM images are, in fact, grain agglomerates, which get fragmented with rise in annealing temperature. In films annealed at 400, 500, and 600 °C, relatively larger particles / grain agglomerates can be seen compared to films annealed at 700 °C, the film morphology appeared most uniform and the particle size also lowest [9, 10].

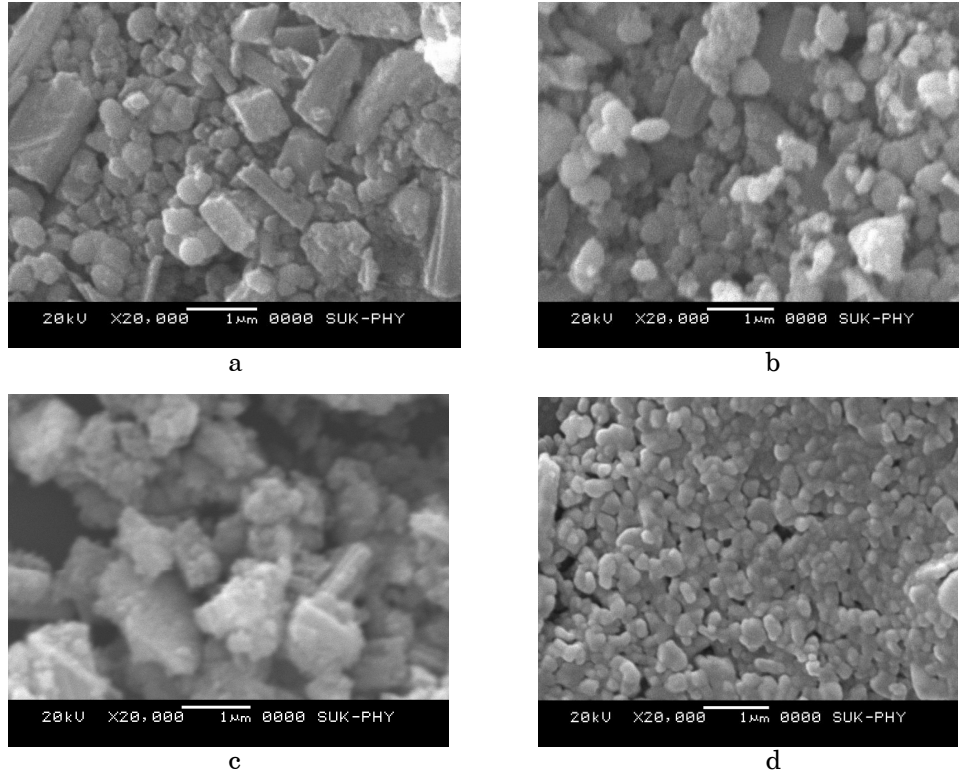


Fig. 4 – SEM image of TiO₂ thin film at different annealing temperatures: (a) 400 °C, (b) 500 °C, (c) 600 °C, and (d) 700 °C

3.3 Electrical Properties

The dc electrical conductivities σ_{dc} of TiO₂ films annealed at 400 - 700 °C as a function of reciprocal temperature were measured in the 300 - 600 K temperature range and their temperature dependence can be fitted to a usual Arrhenius equation:

$$\sigma_{dc} = \sigma_0 \exp(-E_{a\sigma}/k_B T), \quad (1)$$

where $E_{a\sigma}$ is the conductivity activation energy and is k_B Boltzmann constant. The temperature dependence of electrical conductivity (Fig. 5) showed two distinct conduction regions corresponding to two different conduction mechanisms; one, a grain boundary scattering limited and second a variable range hopping [16]. The activation energies of an electrical conduction have been computed for both regions and their variation with annealing temperature is shown in Table 2.

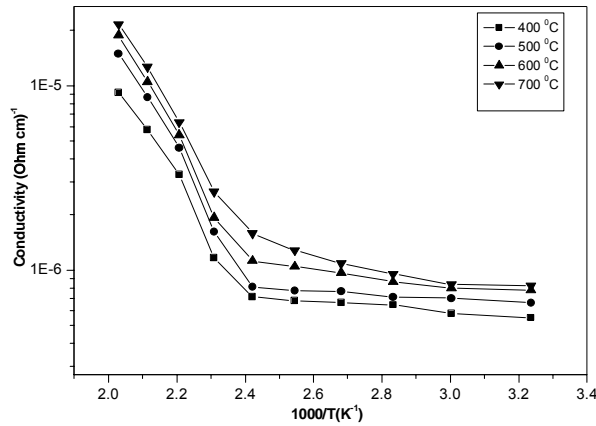


Fig. 5 – Arrhenius plot of dc conductivity vs. $1000/T$ of TiO_2 thin film annealed at (a) 400°C (b) 500°C , (c) 600°C and (d) 700°C for 1 h in air

Table 2 – Effect of annealing on thin film properties of TiO_2

N_0	Annealing temperature, $^\circ\text{C}$	Crystallite Size, nm	Energy gap E_g , eV	Activation energy, E_a eV	
				LT	HT
1	400	50	3.26	0.746	0.195
2	500	54	3.25	0.730	0.202
3	600	59	3.24	0.703	0.180
4	700	60	3.24	0.696	0.190

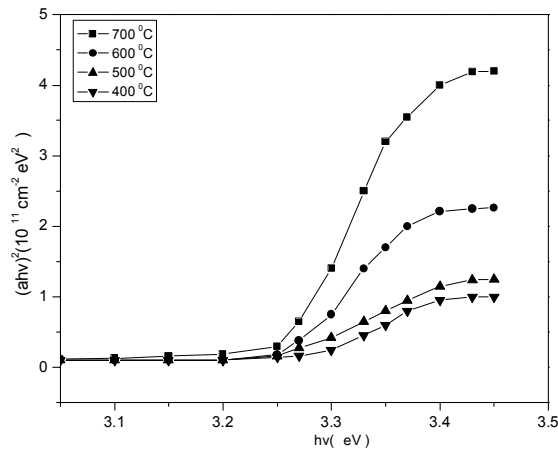


Fig. 6 – Plot of $(ahv)^2$ versus (hv) for different annealing temperatures

3.4 Optical Properties

The optical constants namely absorption coefficient (σ), energy gap (E_g) and the type of the optical transition have been determined by examining an optical absorption spectrum in the 200 - 1000 nm wavelength range at different annealing temperature. Fig. 6 shows determination of the optical

gap from the $(\alpha h\nu)^2$ versus $(h\nu)$ variation in the linear region. The values of optical band gap decreasing slightly with increasing annealing temperature 400 - 700 °C (Table. 2). It is found that the optical absorption coefficient is larger for all the films ($\approx 10^4 \text{ cm}^{-1}$). This may be accounted for the fact that the quality of the TiO_2 film improves when the sample is annealed at a higher temperature (in this case 700 °C). This fact is also by the XRD, SEM images shown in Figs. 1, 4a-d. The $(\alpha h\nu)^2$ versus $h\nu$ plots show straight line behaviour on the higher energy side shows direct type of transitions involved in these films. The type of transitions for TiO_2 films annealed at 400 - 700 °C was confirmed by plotting $\ln(\alpha h\nu)$ versus $\ln(h\nu - E_g)$ variation [17-18].

4. CONCLUSIONS

Nanocrystalline titanium oxide thin films were prepared by sol-gel spin coating techniques on the glass substrate. The effect of annealing temperature on structure, microstructure, morphology, electrical and optical properties of TiO_2 thin films were studied by XRD, HRTEM, AFM, SEM, four probe and UV-Visible measurements. The XRD results reveal that the deposited thin film of TiO_2 has a good nanocrystalline tetragonal mixed anatase and rutile phase structure. The HRTEM, AFM and SEM results demonstrate that a uniform surface morphology and the nanoparticles are fine with an average grain size of about 50 - 60 nm. The dc electrical conductivity found in the range of 10^{-5} to $10^{-6} (\Omega \text{ cm})^{-1}$. Optical studies showed that the TiO_2 has high absorption coefficient ($\approx 10^4 \text{ cm}^{-1}$) with a direct band gap. The optical band gap decreasing slightly with increasing annealing temperature (3.26 - 3.24 eV).

The author (VBP) thankful to Department of Science and Technology, Government of India, New Delhi for sanctioning Fast Track Project (SR/FTP/PS-09/2007).

REFERENCES

1. R.S. Singh, V.K. Rangari, S. Sanagapalli, V. Jayaraman, S. Mahendra, V.P. Singh, *Sol. Energ. Mat. Sol. C.* **82**, 315 (2004).
2. J. Sabataityte, I. Oja, F. Lenzmann, O. Volobujeva, M. Krunk, *CR Chim.* **9**, 708 (2006).
3. S.S. Madaeni, N. Ghaemi, *J Membrane Sci.* **303**, 221 (2007).
4. A.R. Gandhe, J.B. Fernandes, *J Solid. State Chem.* **178**, 2953 (2005).
5. K.B. Sundaram, A. Khan, *Thin Solid Films* **295**, 87 (1997).
6. J. Aranovich, A. Ortiz, R.H. Bube, *J. Vac. Sci. Technol.* **16**, 994 (1979).
7. M.N. Islam, M.O. Hakim, H. Rahman, *J. Mater. Sci.* **22**, 1379 (1987).
8. S. Major, K.L. Chopra, *Solar Energ. Mater.* **17**, 319 (1988).
9. M. de la L. Olvera, A. Maldonado, R. Asomoza, M. Konagai, M. Asomoza, *Thin Solid Films* **229**, 196 (1993).
10. K. Kamata, S. Matsumoto, P. Souleite, B.W. Wessels, *J. Mater. Res.* **3**, 740 (1988).
11. Y. Natsume, H. Sakata, T. Hirayama, H. Yanagida, *J. Appl. Phys.* **72**, 4203 (1992).
12. W. Tang, D.C. Cameron, *Thin Solid Films* **238**, 83 (1994).
13. V. Craciun, J. Elders, J.G.E. Gardeniers, I.W. Boyd, *Appl. Phys. Lett.* **65**, 2963 (1994).
14. M.M.A. Sekkina, A. Tawfik, M.I. Abd El-Ati *Thermochimica Acta*, **86**, 59 (1985).
15. S. Chandra, R.K. Pandya, *Phys. Status Solidi A* **72**, 415 (1982).
16. K.L. Narasimhan, S.P. Pai, V.R. Palkar, R. Pinto, *Thin Solid Films* **295**, 104 (1997).
17. A.P. Roth, D.F. Williams, *J. Appl. Phys.* **52**, 6685 (1981).